



INTERNATIONAL ATOMIC ENERGY AGENCY
 UNITED NATIONS EDUCATIONAL, SCIENTIFIC AND CULTURAL ORGANIZATION
INTERNATIONAL CENTRE FOR THEORETICAL PHYSICS
 I.C.T.P., P.O. BOX 586, 34100 TRIESTE, ITALY, CABLE: CENTRATOM TRIESTE



SMR. 767 - 3

**MINIWORKSHOP ON STRONG CORRELATIONS
 AND QUANTUM CRITICAL PHENOMENA
 (4 - 22 July 1994)**

=====

**UNIVERSAL MAGNETIC PROPERTIES OF
 QUANTUM ANTIFERROMAGNETS**

Andrey V. CHUBUKOV
 P.L. Kapitza Institute for Physical Problems
 117334 (GSP-1) Moscow, Russian Federation
 Present Address:
 Physics Department
 University of Wisconsin
 53706 Madison, Wisconsin, USA

=====

These are preliminary lecture notes, intended only for distribution to participants.

=====

PART I

Weakly doped quantum antiferromagnets

Andrey V. Chubukov

Univ. of Wisconsin

Collaborators:

Subir Sachdev / Yale

David Frenkel / U. of Houston

Karen Muraelian / U. of Wisconsin

Sasha Sokol / U. of Illinois

Plan

★ Half-filling (lecture 1)

Heisenberg AFM, quantum-classical crossover

★ Low doping (lecture 2)

SDW description

- pockets of holes
- uniform susceptibility
- spin stiffness
- incommensurability in $\text{La}(\text{Sr})\text{CuO}$

★ How long in doping can we extend SDW description

Universal magnetic behavior

in $\text{La}_{2-x}\text{Sr}_x\text{CuO}_4$

Andrey Chubukov

University of Wisconsin - Madison

Sabir Sachdev

Yale University

Plan

★ Introduction:

La_2CuO_4 as 2D antiferromagnet

★ Classical approach (Chakravarty, Halperin & Nelson)

possibility for a new behavior above 600K

★ Quantum-critical approach

- uniform susceptibility
- structure factor
- correlation length
- spin-lattice relaxation rates, T_1 ; T_2
- magnetism vs doping

★ Conclusions





Large La_2CuO_4 crystals the antiferromagnetic parent compound of a family of cuprate superconductors mounted on a goniometer for inelastic neutron-scattering studies of spin excitations. These plate-like crystals are grown by Sang-Wook Cheong (AT&T Bell Laboratories) and Zachary Fisk (Los Alamos National Laboratory) using a Cl_2 solvent flux technique. The in-plane size reaches up to 8–10 cm. **Figure 1**

are very similar despite T_c 's that differ by as much as a factor of five.

Electronic states and Fermi surface

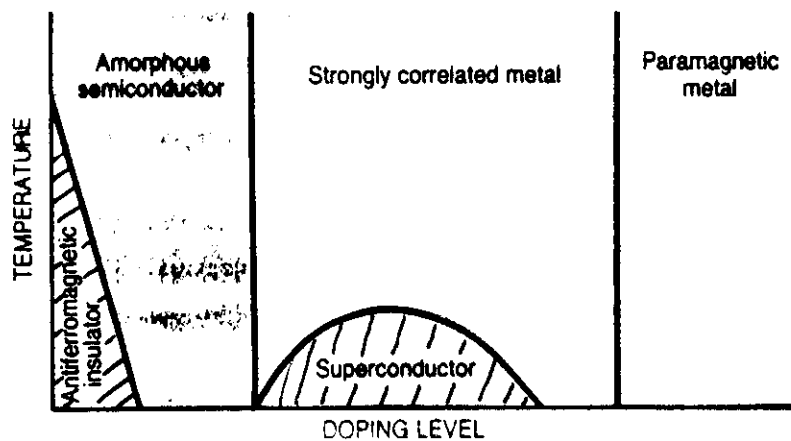
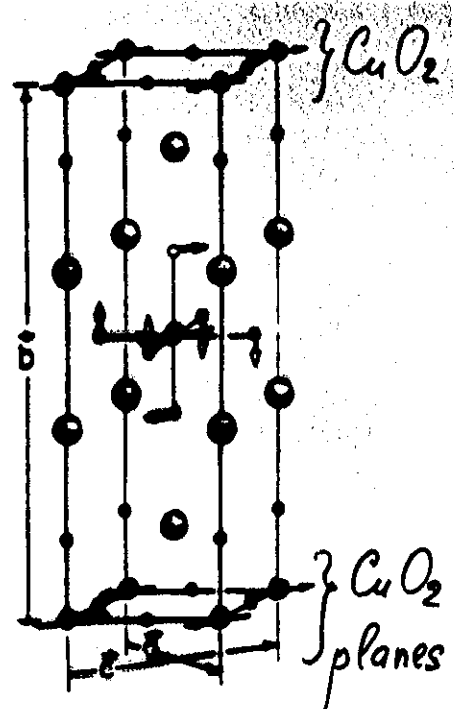
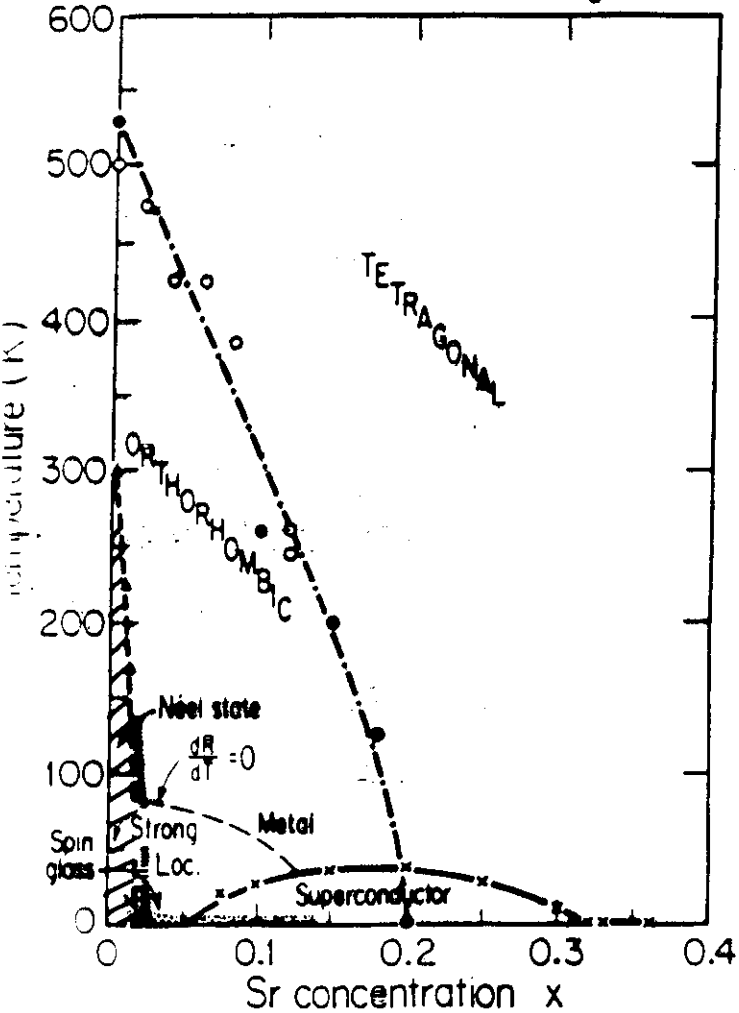
An initial question concerns the nature of the electronic states near the Fermi energy E_F , which are responsible for the transport properties. Bonding between nominal Cu^{2+} and O^{2-} has both ionic and covalent character and involves the $\text{Cu } 3d$ and $\text{O } 2p$ orbitals. The origin of the covalency is ultimately rooted in the proximity in energy of the $3d$ and $2p$ levels, and thus it is specific to the combination of these two elements. A similar energy degeneracy occurs between the $6s$ levels of Pb and Bi and the $2p$ level of O in the BaBiO_3 , PbO_2 superconductors. Various types of electron spectroscopies confirm this covalent mixing and reveal that the highest occupied electronic states—the ones near E_F —have both $3d$ and $2p$ character, with a predominance of the latter. Consequently, the holes introduced in the CuO_2 layers by doping are not located only at the Cu sites, or only at the O sites, but have a mixed character.

More important is the question of the existence of a Fermi surface and its shape. The Fermi surface is the locus in momentum space where the occupation of the

electronic states drops abruptly and where the energy required to create particle-hole excitations vanishes. In a simple metal, with a spherical Fermi surface, at $T = 0$ all states with momentum k less than the Fermi momentum k_F are filled, and states with $k > k_F$ (and hence energy $E > E_F$) are empty. In general, the shape of the Fermi surface is determined by the momentum dependence of electronic energies $E(\mathbf{k})$, also called electronic band structure. $E(\mathbf{k})$ is material specific, and great advances have been made in calculating $E(\mathbf{k})$ even for complicated compounds such as the cuprates. When one considers the strong correlations among the electrons in the cuprates, the existence of a Fermi surface is not obvious.

Photoemission electron spectroscopy is one of the experimental tools used to study $E(\mathbf{k})$. The emission intensity is measured as a function of energy and emission angle along the principal symmetry directions of the crystal. The best results available are for $\text{Bi}_2\text{Sr}_2\text{CaCu}_2\text{O}_8$, for which cleaving in a vacuum produces clean and chemically stable surfaces. The main result is that the measured energy bands $E(\mathbf{k})$ cross the Fermi energy at points in \mathbf{k} space that are given by the calculations, confirming the presence of a Fermi surface. In addition, more subtle but important details of the emission spectra

La_{2-x}Sr_xCuO₄ Phase Diagram

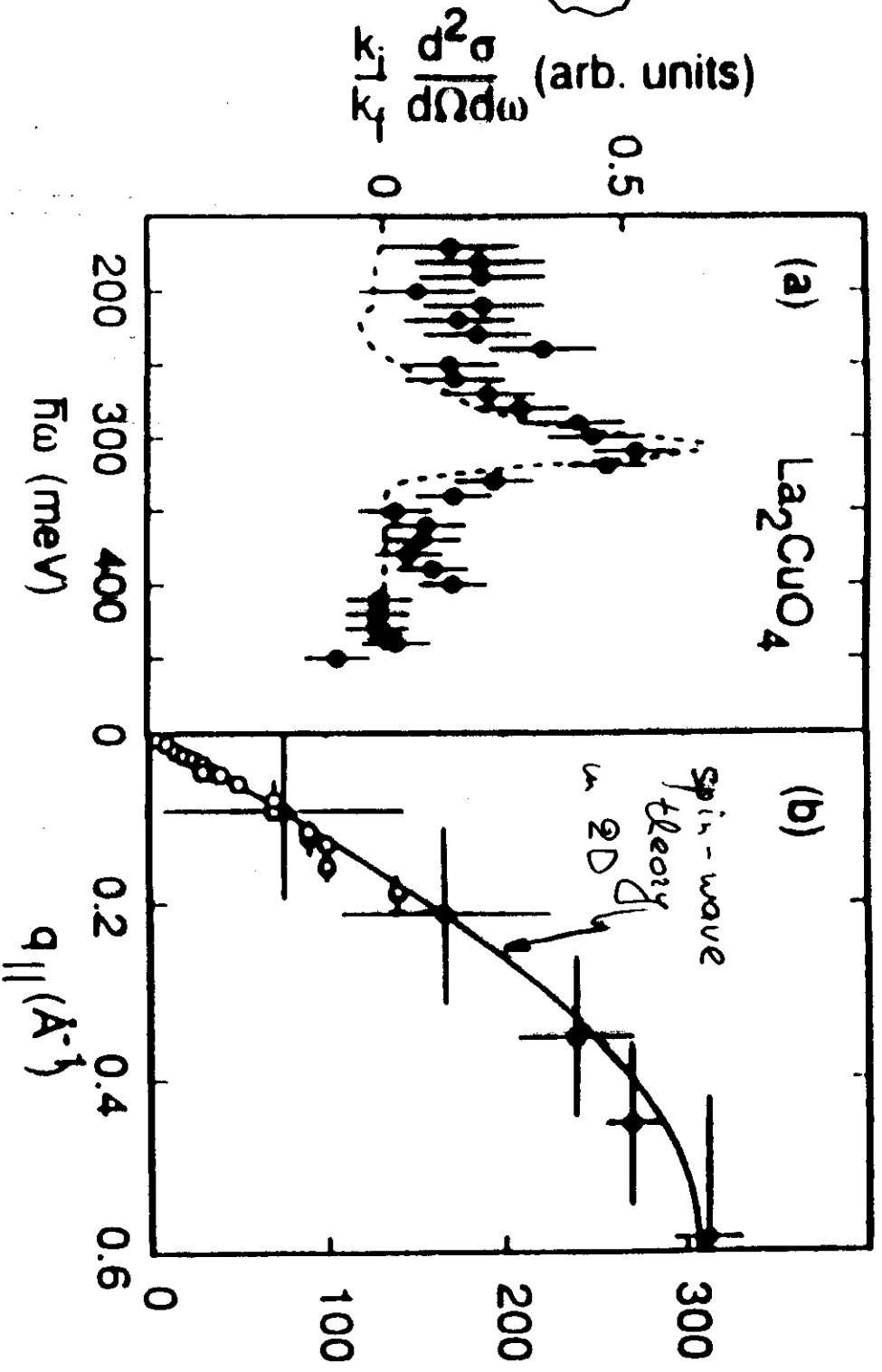


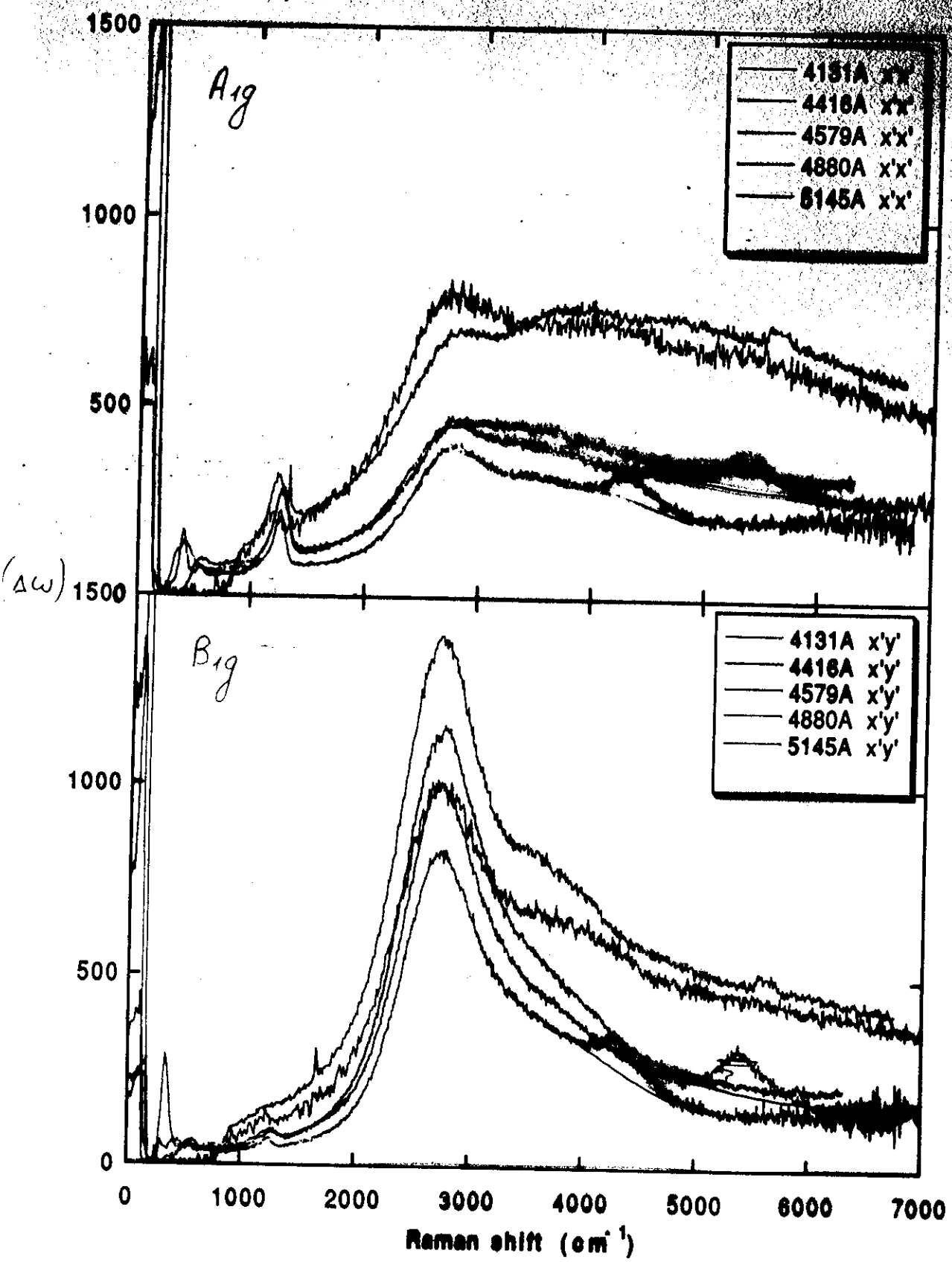
$$J = 0.13 \pm 0.01 \text{ eV}$$

Raman scattering

gives

$$J = 0.128 \text{ eV}$$





$\Delta\omega$

For ordered antiferromagnet

for $\vec{k} \approx (\pi, \pi)$

$$\chi(q, \omega) = \frac{N_0^2}{\rho_s q^2 - \chi_{\perp} \omega^2} \quad \vec{q} = (\pi, \pi) - \vec{k}$$

ρ_s - spin stiffness

χ_{\perp} - transverse susceptibility

$$c^2 = \rho_s / \chi_{\perp}$$

N_0 ordered moment (sublattice magnetization)

2D magnetism

• long-range order at $T=0$ (even for $S=1/2$)
 $\rho_s > 0$

• no LRO and no phase transitions at finite T

(thermal fluctuations produce internal scale)

$$\chi = 0.34 \left(\frac{\hbar c}{2\pi \rho_s} \right) \exp \left(\frac{2\pi \rho_s}{\hbar k_B T} \right) \quad 2\pi \rho_s \gg T$$



(Chakravarty et al; 88, 89)

(Hasenfratz et al; 90; 91)

2D $S=1/2$ square-lattice AFM

$$c = 1.67 \text{ J}$$

spin-wave velocity

$$\rho_s = 0.18 \text{ J}$$

spin stiffness

$$N_0 = 0.305$$

AFM moment

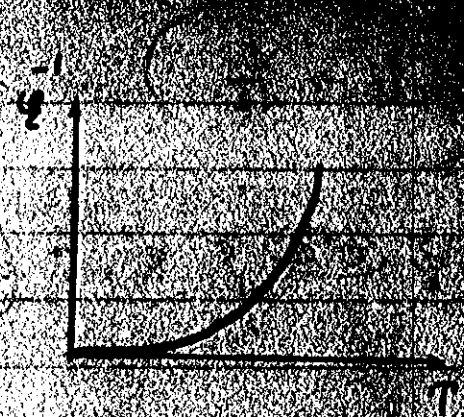
Singh, 89

Igarashi, 92

$$(2\pi \rho_s \gg 1)$$

correlation length

$$\xi^{-1} \sim \exp\left\{-\frac{2\pi\rho_s}{T}\right\}$$

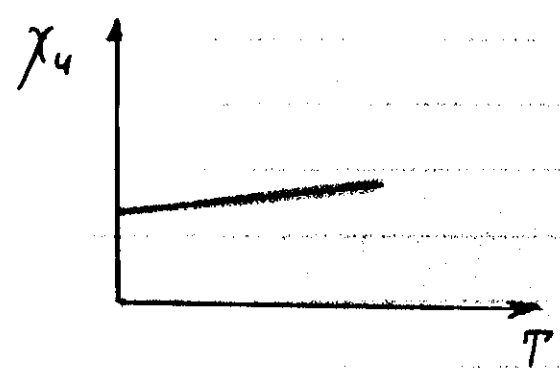


(Chakravarty et al.)

uniform susceptibility

$$\chi_u = \frac{2}{3} \chi_{\perp}^{T=0} + \frac{1}{3\pi} \frac{k_B T}{c^2}$$

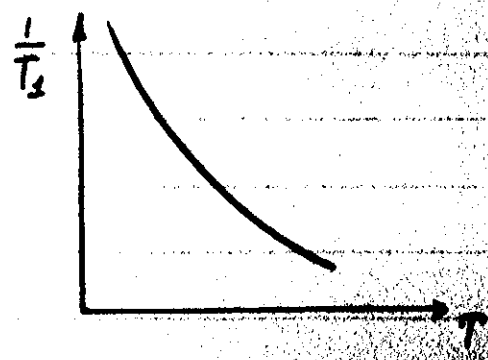
(Chubukov & Sachdev,
Hosenzrate & Niedermayer)



spin-lattice relaxation rate

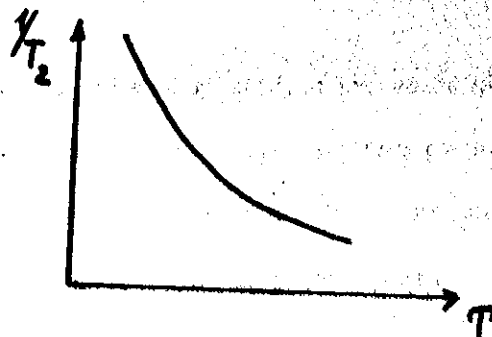
$$\frac{1}{T_1} \sim \frac{T}{\omega} \int d^3q \chi''(q, \omega) \Big|_{\omega \rightarrow 0} \sim T^{3/2} \xi$$

(Chakravarty & Orbach)



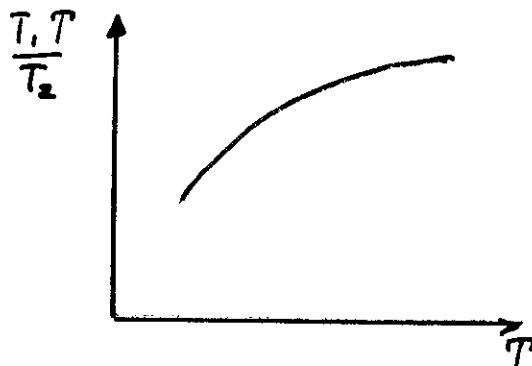
spin-lattice decay rate (Sokol & Pines)

$$\frac{1}{T_2} \sim \left(\int d^2q \chi^2(q, 0) \right)^{1/2} \sim T^{\frac{1}{2}}$$

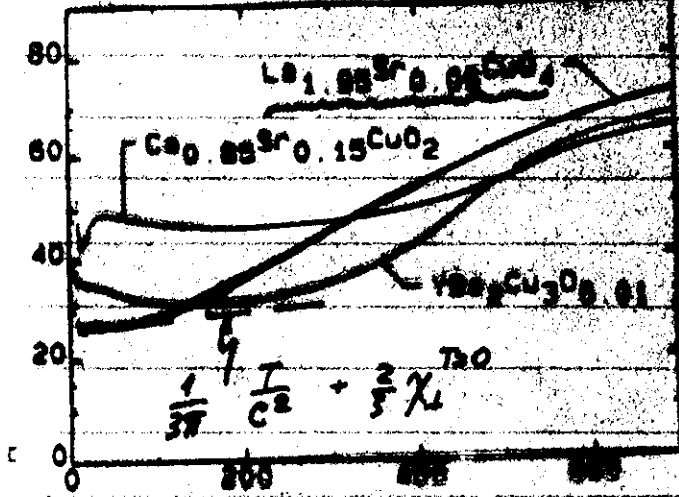


ratio of $\frac{T_1}{T_2}$

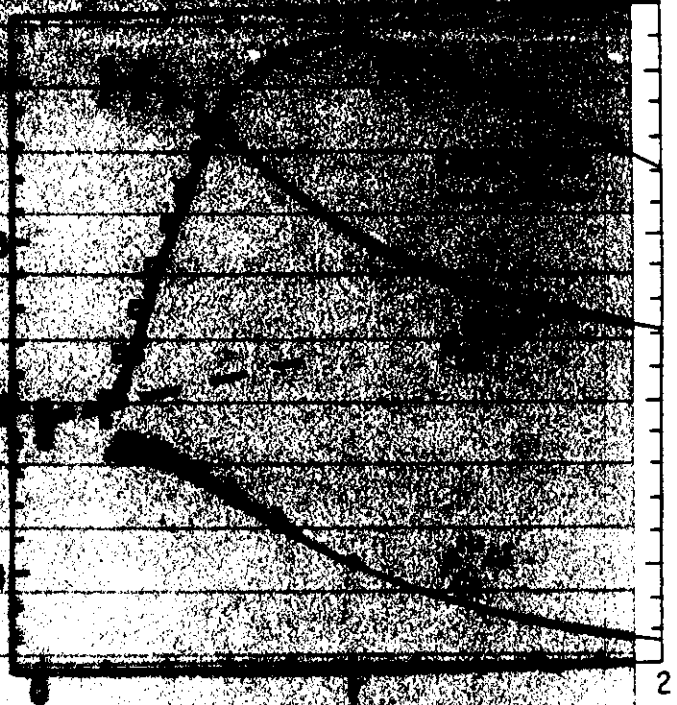
$$\frac{T_1}{T_2} \sim T^{\frac{1}{2}}$$



Uniform susceptibility

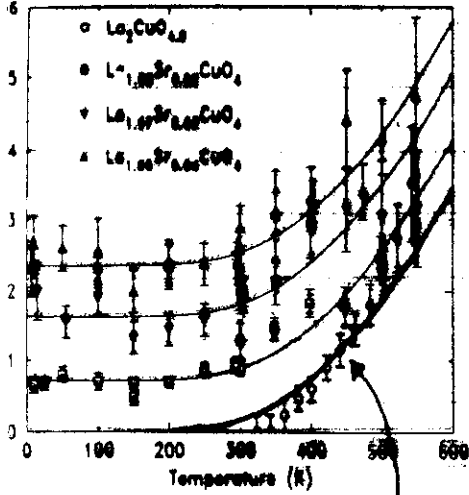


Johnston et al



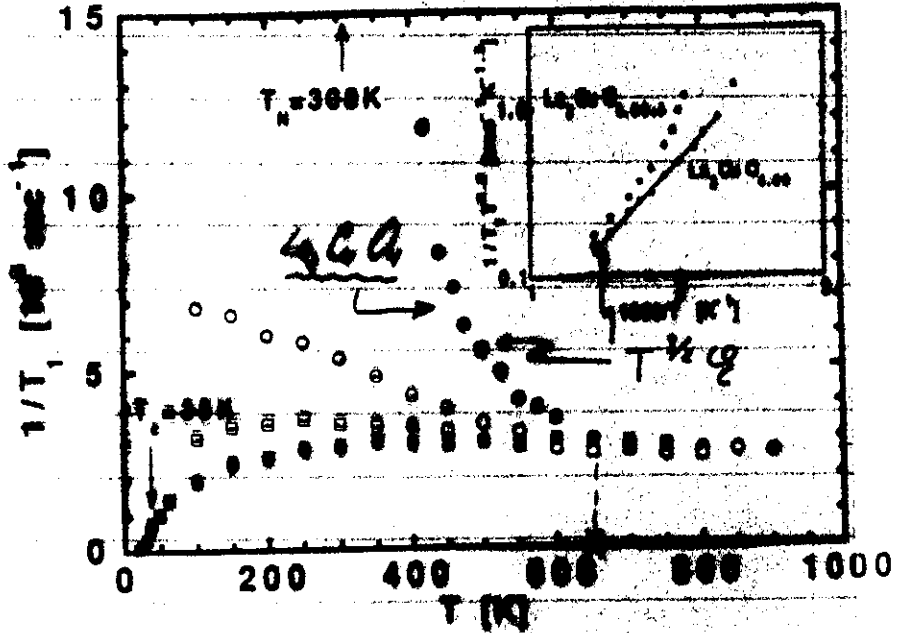
Singh & Gelfand,
Ding & Makivic

Inverse Magnetic Correlation Length



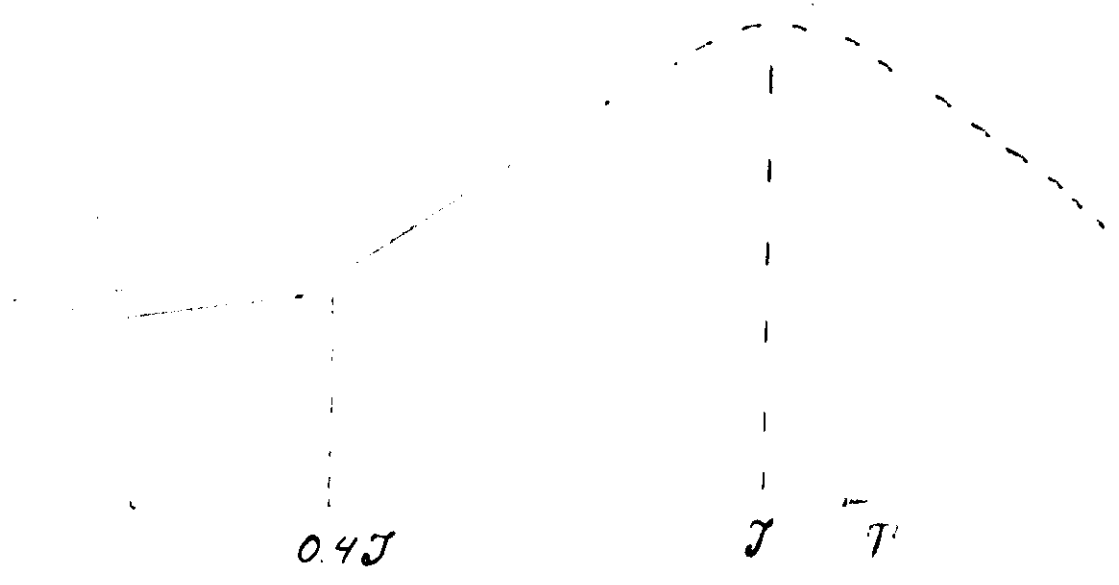
Keimer et al

$$\xi^{-1} \sim \exp\left\{\frac{A}{T}\right\}$$

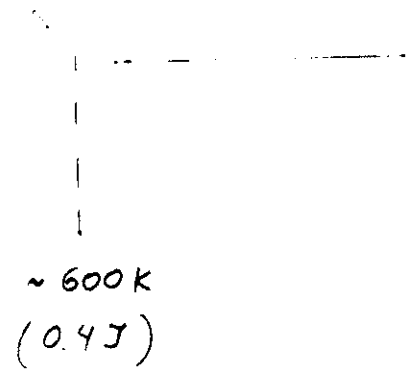


Imai et al

▲



▲



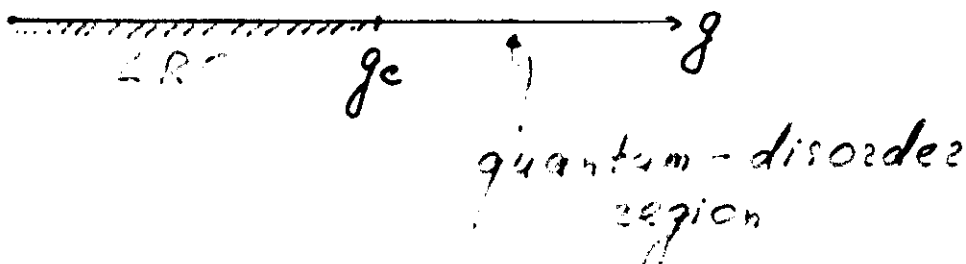
★ Possibility for another type of behavior at intermediate T , $0.4T < T < 0.6J$

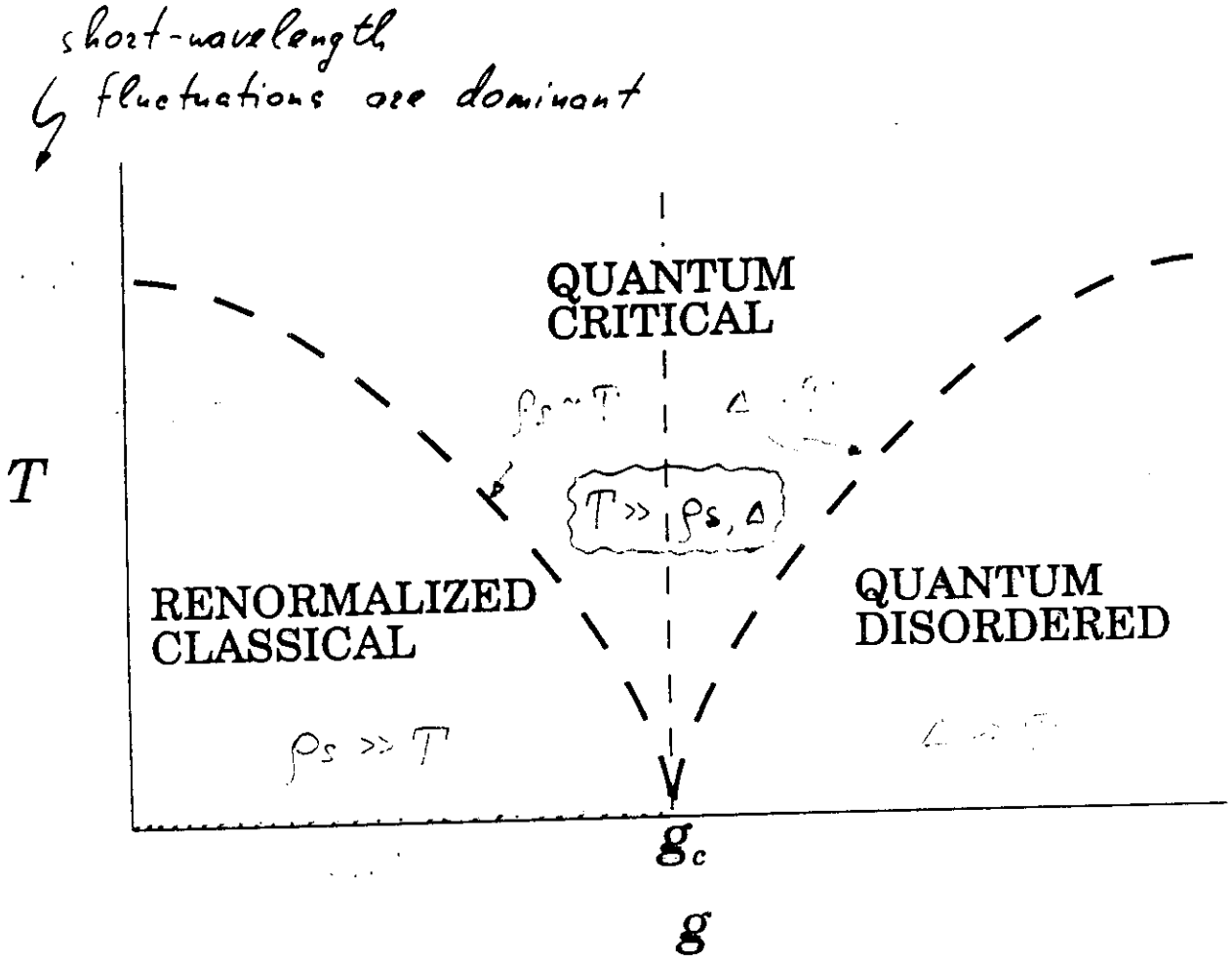
$$600 \text{ K} < T < 900 \text{ K} \quad (\text{pure } \text{La}_2\text{CuO}_4)$$

- no phase transitions at $T \neq 0$, only smooth crossover (in 2D)

★ We never considered the role of quantum fluctuations (apart from renormalization of ρ_s, c)

- let g measure the strength of quantum fluctuations
($g \sim 1/s$ at $S \gg 1$)





We argue: that most of experiments on uniform susceptibility, T_1 and T_2 are done in the quantum-critical region

Chubukov & Sachdev, 93

To this end, we consider
antiferromagnets which have

$T \ll J$, $\rho_s \ll J$ but T/ρ_s arbitrary
(on the ordered side)

$T/\rho_s \ll 1$ ren-classical region

$T/\rho_s \gg 1$ quantum-critical region

- The system realizes (at $\rho_s \ll J$) that it is
not at the critical point only at
very large scales \Rightarrow universality!

- we can use scaling

 $\rho_s = \frac{\hbar c}{\xi_J} \times (\text{number})$ $\xi_J \sim (g_c - g)^{-\nu}$

 at $\rho_s = 0$, $L \xi = \frac{\hbar c}{T}$

"finite size" of a critical
theory

From general principles of scaling
 any observable is a function of
 three dimensionless quantities

$$\bar{k} = k L t$$

$$\bar{\omega} = \frac{\omega}{c} L t$$

$$X = \frac{L}{\lambda_0}$$



$$\bar{k} = \frac{k c k}{T}$$

$$\bar{\omega} = \frac{\omega}{T}$$

$$X = \frac{N T}{2 \pi p s}$$

N - number of
 components of the
 order parameter
 ($N=3$ for AFM)

Scaling predictions for the

$$\star \chi_u(\tau) \sim \tau$$

$$\star \Psi(\tau) \sim 1/\tau$$

$$\star 1/T_2 \sim \tau^p$$

$$\star 1/T_2 \sim \tau^{-1+\eta}$$

$$\left. \begin{array}{l} \star 1/T_2 \sim \tau^p \\ \star 1/T_2 \sim \tau^{-1+\eta} \end{array} \right\} p = 2.01 \pm 0.1$$

$$\frac{T_1 \tau}{T_2} = \text{const}$$

$$\star S(k) \sim \tau^{\eta-1} f(c k / \tau)$$

$$\star \chi_L''(\omega) \sim \tau^\eta \varphi(\omega / \tau)$$

$$\int \frac{d^3 q}{4\pi^3} \chi''(q, \omega)$$

$$\chi_S(k, \omega) = \frac{N_0^2}{\rho_S} \left(\frac{\hbar c}{k_B T} \right) \left(\frac{k_B T}{2\pi \rho_S} \right)^\eta \Psi(\bar{k}, \bar{\omega}, x)$$

Calculation of universal functions

RG approach - perturbative expansion around ordered state (only transverse fluctuations)

We use $1/N$ expansion for $O(N)$ δ -model;

$N=3$ is a goal.

Disadvantage : no "real" small parameter for the expansion

Advantage : the starting point is a mean-field solution for the Green function

$$G = \frac{1}{k^2 + \omega^2 + m_0^2}$$

\Rightarrow this implies that the symmetry is unbroken

We do not have to separate classical and quantum fluctuations.

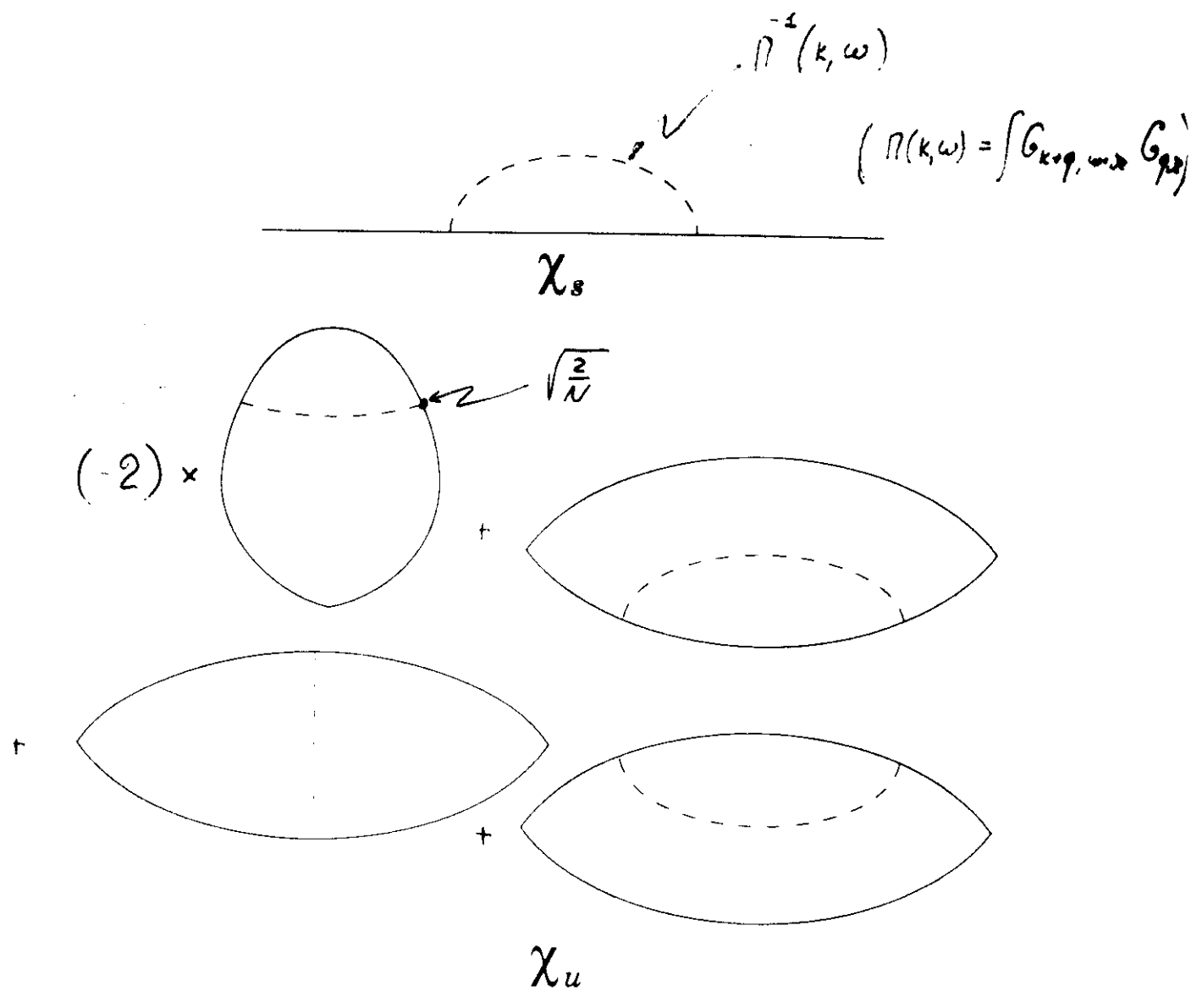


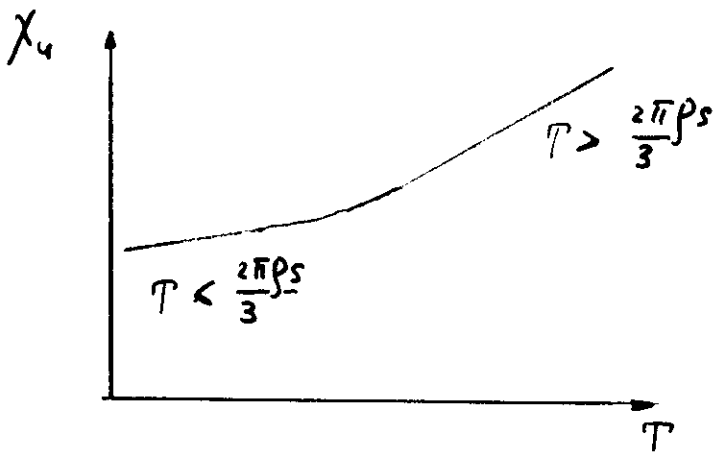
FIG 6.

Uniform susceptibility

$$\chi_u(T) = \left(\frac{g \mu_B}{k_B} \right)^2 \bar{\chi}$$

$$\bar{\chi} = \begin{cases} 0.66 \chi_{\perp}^{T=0} + 0.11 \frac{T}{c^2} & T \ll \frac{2\pi\beta_S}{3} \\ 0.4 \chi_{\perp}^{T=0} + 0.2T \frac{T}{c^2} & T \gg \frac{2\pi\beta_S}{3} \end{cases}$$

quantum-critical result (obtained in $\frac{1}{N}$ expansion, $N=3$ is the goal)



Slopes

- renormalised - classical

$$0.11 = \frac{1}{\pi} \frac{N-2}{N}$$

- quantum - critical

$$0.27 = \underbrace{\frac{\sqrt{5}}{\pi} \log \frac{\sqrt{5}+1}{2}}_{0.34} \left(1 - \frac{0.62}{N}\right)$$

our $N = \infty$ result is two times larger than in
mean-field Schwinger-boson approach

■ Monte-Carlo, High T series expansion

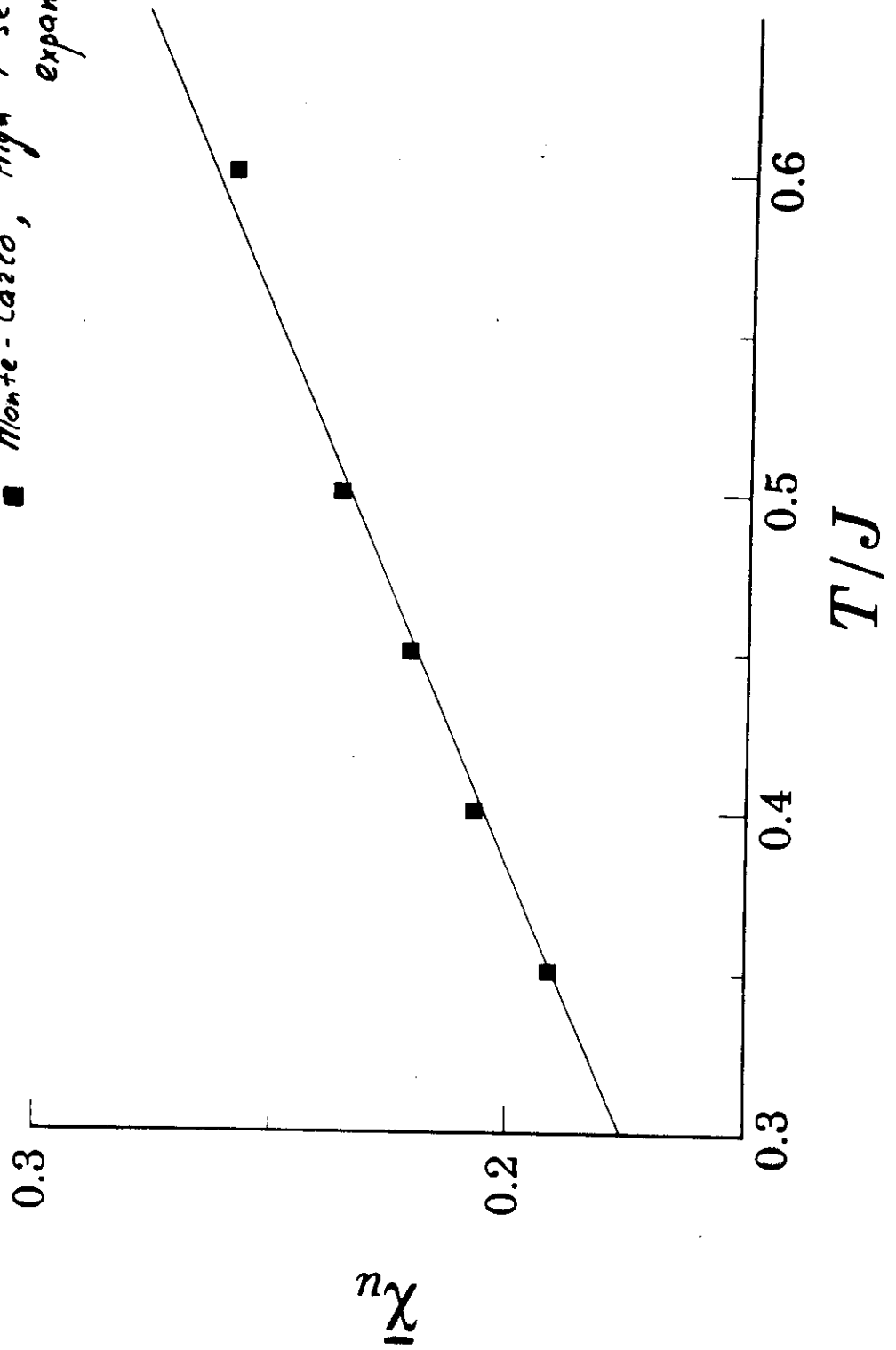


FIG 7

PART II

Ren.- classical

Quantum -
critical

χ_u
uniform susceptibility

$$0.66 \chi_{\perp}^{T=0} + 0.11 \frac{T}{C^2}$$

$$0.4 \chi_{\perp}^{T=0} + 0.27 \frac{T}{C^2}$$

ξ
correlation length

$$\sim e^{2\pi\beta S/T}$$

$$\sim 1/T$$

$1/T_3$
spin-lattice
relaxation rate

$$\sim T^{3/2} \xi$$

$$\sim T^? \approx \text{const}$$

$1/T_2$
spin-lattice
decay rate

$$\sim T \xi$$

$$\sim T^{-1+\eta} \approx T^{-1}$$

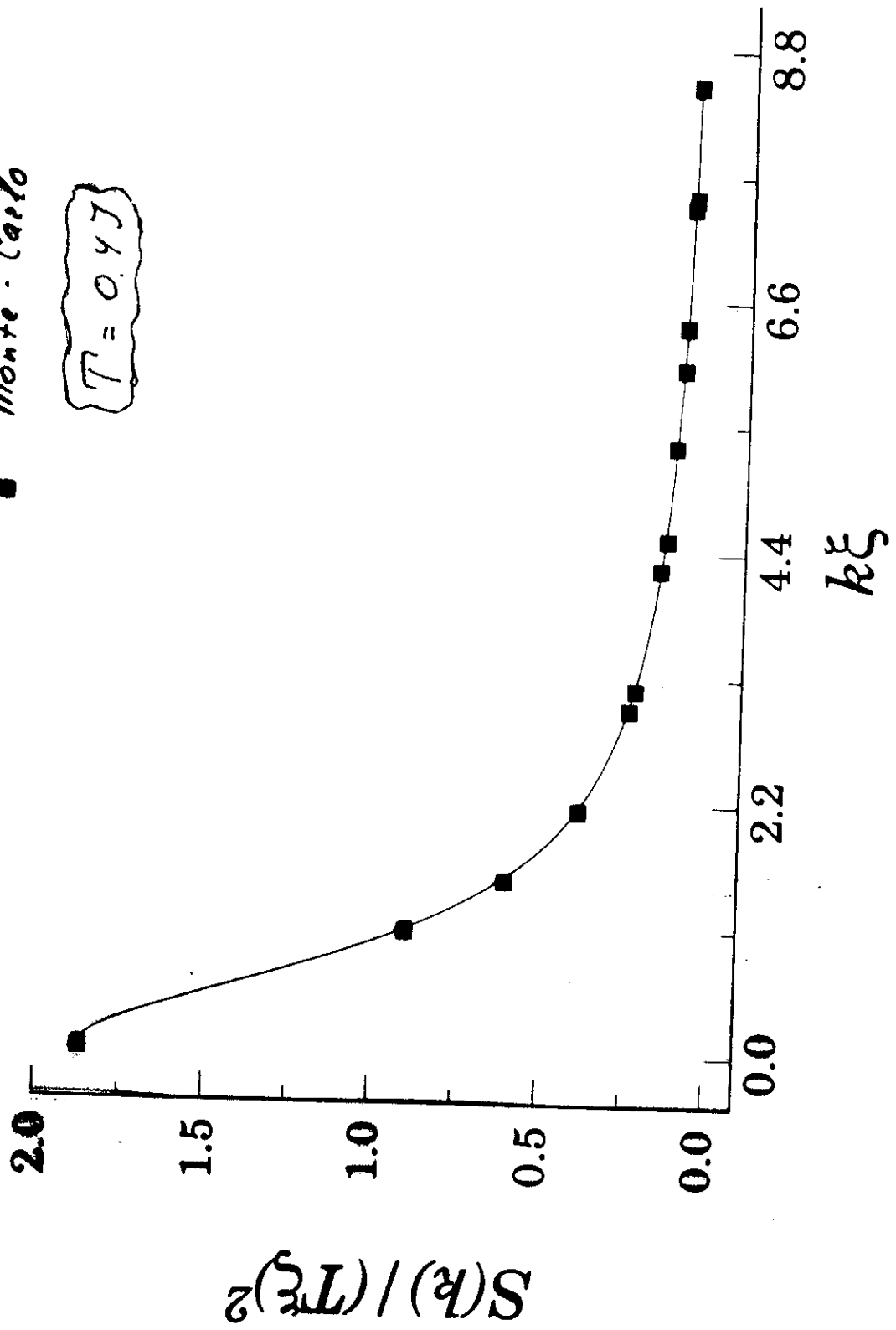
$$\frac{T_1 T}{T_2}$$

$$\sim T^{1/2}$$

const

■ Monte-Carlo

$T = 0.4 J$



Crossover temperature

- In the large- N expansion:

$$X = \frac{2\pi\beta_s}{NT}$$

$X > 1$ classical region

$X < 1$ quantum-critical

$$\beta_s = 0.18 \text{ J}, \quad N = 3 \quad \Rightarrow \quad X = \frac{T_{c2}}{T}, \quad T_{c2} \sim 0.38 \text{ J} \sim \underline{\underline{600 \text{ K}}}$$

∴ Deep in the ren-classical region, one has (at arbitrary N)

$$\mathcal{Q} \sim \exp\left[\frac{2\pi\beta_s}{(N-2)T}\right]$$

Formally, the expansion holds in $\frac{2\pi\beta_s}{T} \sim \frac{\bar{T}_{c2}}{T}$,

$$\bar{T}_{c2} \sim 1.13 \text{ J} \sim 1700 \text{ K}$$

- We found in $\frac{1}{N}$ expansion, that
 $N \rightarrow N-2$ substitution results from
 the series of $\frac{1}{N} \log(T\varphi)$ terms as
 \Rightarrow it holds only if $\log(T\varphi) \gg 1 \Rightarrow \rho \approx T(\varphi)$

$$T\varphi \sim e^{\frac{2\pi\rho_S}{(N-2)T}} \rightarrow e^{\frac{2\pi\rho_S}{NT}} e^{\frac{4\pi\rho_S}{N^2T}}$$

$$\rightarrow e^{\frac{2\pi\rho_S}{NT}} \left[1 + \frac{1}{N} \frac{2\pi\rho_S}{NT} + \dots \right]$$

$$\log T\varphi_0 = \frac{2\pi\rho_S}{NT}, \quad \text{therefore}$$

"N=∞" result

$$T\varphi = (T\varphi_0) \left[1 + \frac{1}{N} \log T\varphi_0 + \frac{1}{2N^2} \log^2 T\varphi_0 + \dots \right. \\ \left. + \frac{1}{N} \times \text{const} + \dots \right]$$

[] this is what we obtain in $\frac{1}{N}$ expansion

• longitudinal relaxation, $1/T_1$

$$\mathcal{H} = \sum_{\mathbf{r}} I_{\mathbf{r}} S_{\mathbf{r}'} A_{\mathbf{r},\mathbf{r}'} \equiv \sum_{\mathbf{r}} I_{\mathbf{r}} \times H_{\text{eff}}(\mathbf{r})$$

$$H_{\text{eff}} = \sum_{\mathbf{r}'} S_{\mathbf{r}'} A_{\mathbf{r},\mathbf{r}'}$$

In general, $H_{\text{eff}}(\mathbf{r}, t)$

Suppose, we apply transverse oscillating field with ω_0

$$1/T_1 \sim \int dt \langle H_{\text{eff}}(\mathbf{r}, t) H_{\text{eff}}(\mathbf{r}, 0) \rangle e^{i\omega_0 t}$$

$$1/T_1 \sim A^2 \int d\mathbf{k} S(\mathbf{k}, \omega_0)$$

• transverse relaxation, $1/T_2$

$$\mathcal{H} = \sum_{\mathbf{r}} I_{\mathbf{r}} S_{\mathbf{r}'} A_{\mathbf{r},\mathbf{r}'} \Rightarrow \sum_{\mathbf{r}'} S_{\mathbf{r}'} H_{\text{eff}}(\mathbf{r}')$$

$$H_{\text{eff}}(\mathbf{r}') = \sum_{\mathbf{r}} I_{\mathbf{r}} A_{\mathbf{r},\mathbf{r}'} \Rightarrow H_{\text{eff}}(\mathbf{q}) \Rightarrow \tilde{S}(\mathbf{q}) = \chi'(\mathbf{q}) H_{\text{eff}}(\mathbf{q})$$

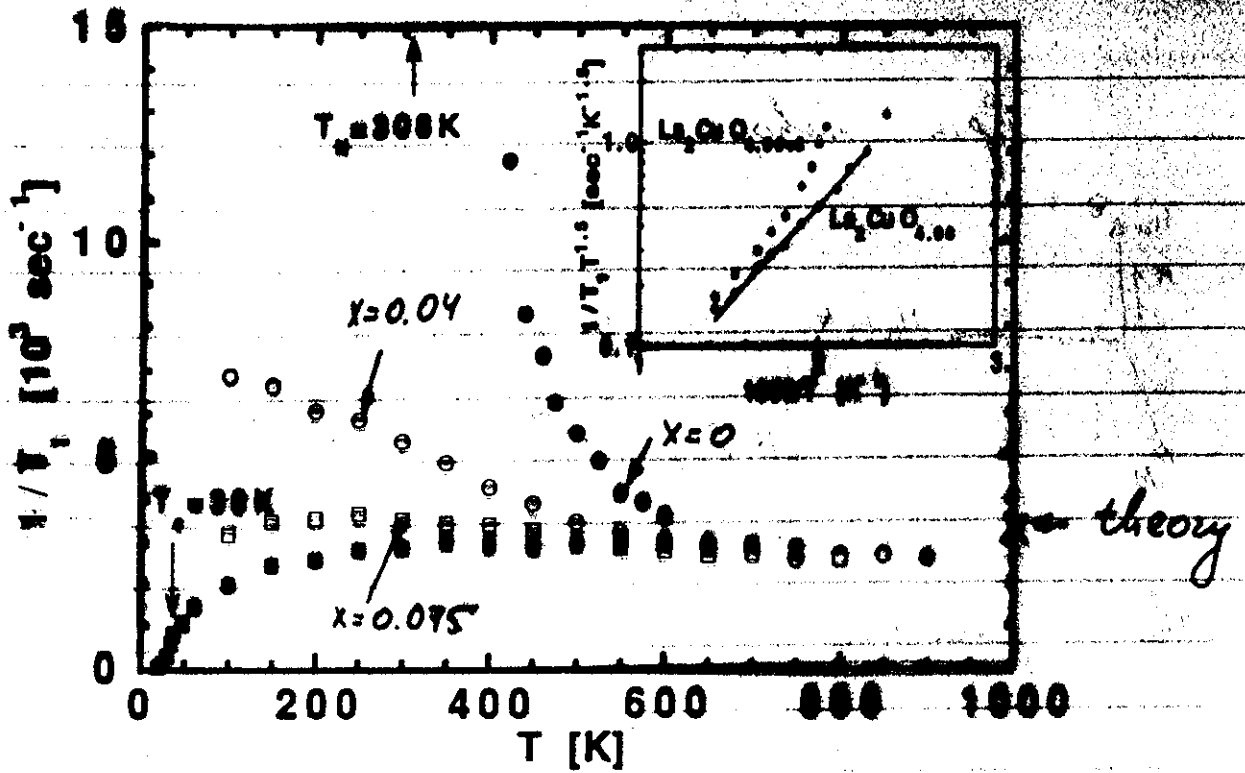
$$\Rightarrow \tilde{S}(\mathbf{r}) \Rightarrow \mathcal{H} = A_{\mathbf{r},\mathbf{r}'} \tilde{S}_{\mathbf{r}} I_{\mathbf{r}} \quad \uparrow \text{polarization}$$

$$H_{\text{eff}} = \sum_{\langle ij \rangle} a_{ij} I_i I_j$$

$$a_{ij} \sim A^2 \chi'$$

spin-echo technique : signal(t) $\sim e^{-t^2/2t^2}$; $\frac{1}{t^2} = \sum_{\mathbf{k}} a_{\mathbf{k}}^2$

$$1/T_1 \sim \int d^2q \frac{\chi''(q, \omega)}{\omega} \Big|_{\omega \rightarrow 0}$$



Theory (quantum-critical)

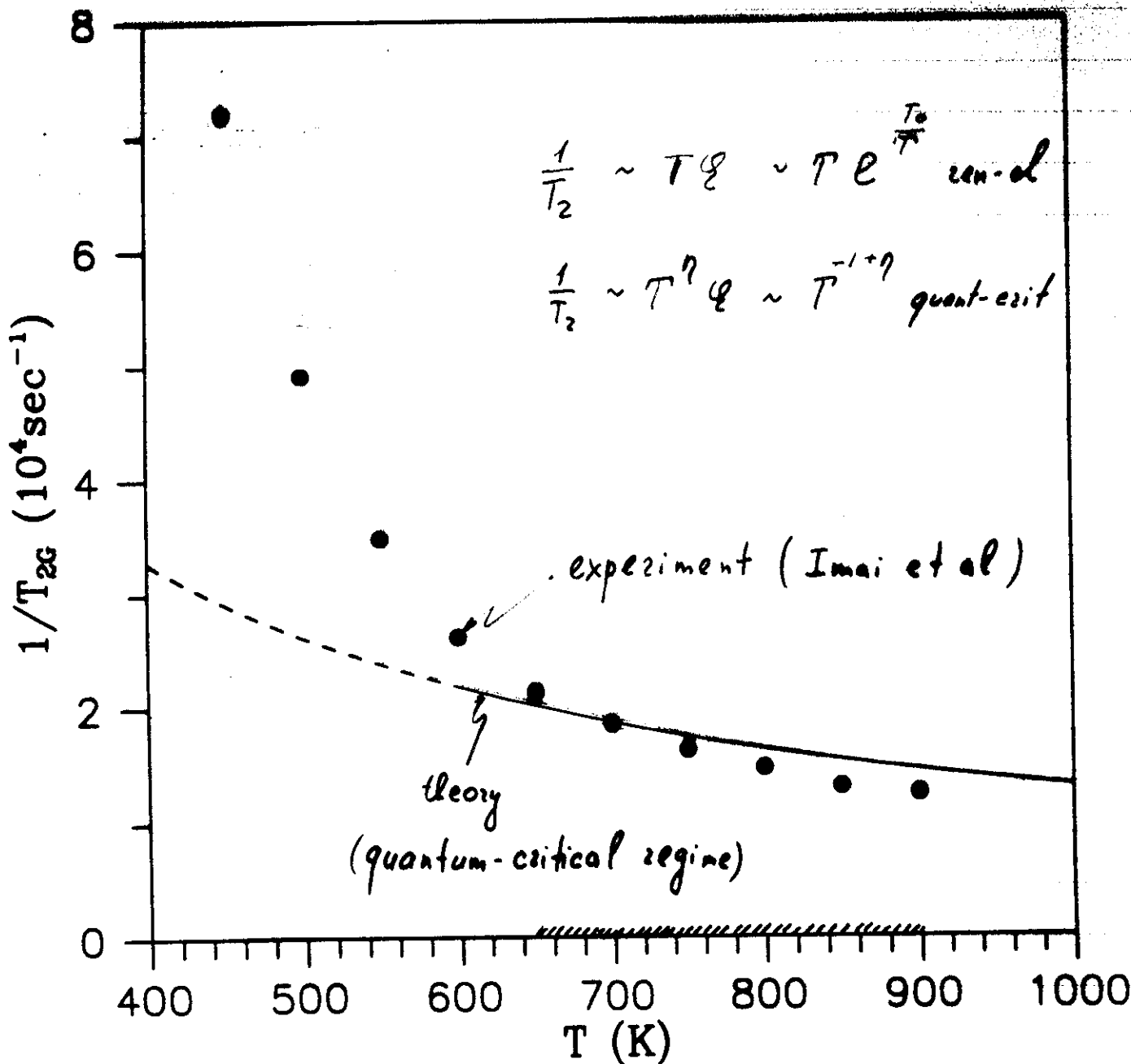
$$1/T_1 \approx 3.2 \pm 0.5 \times 10^3 \text{ sec}^{-1}$$

experiment

$$1/T_1 \approx 2.7 \cdot 10^3 \text{ sec}^{-1} \text{ at } T \approx 700 \text{ K}$$

Spin-echo decay rate, $1/T_2$

$$1/T_2 \sim \left[\int d^3q \chi^2(q, 0) \right]^{1/2}$$



Chubukov, Sachdev & Sokol

Explicit calculations of T_2 vs N

$$\frac{1}{T_2} = \frac{A^2}{4\pi} \left(\frac{N_0^2}{\rho_s} \right) \left(\frac{N T}{2\pi \rho_s} \right)^2 \frac{1}{a}$$

$$\times \left(1 + \frac{0.46}{N} \right)$$

$$\bar{Q}^{-1}(T) = 0.962 \frac{T}{hc} \left(1 + \frac{0.237}{N} \right)$$

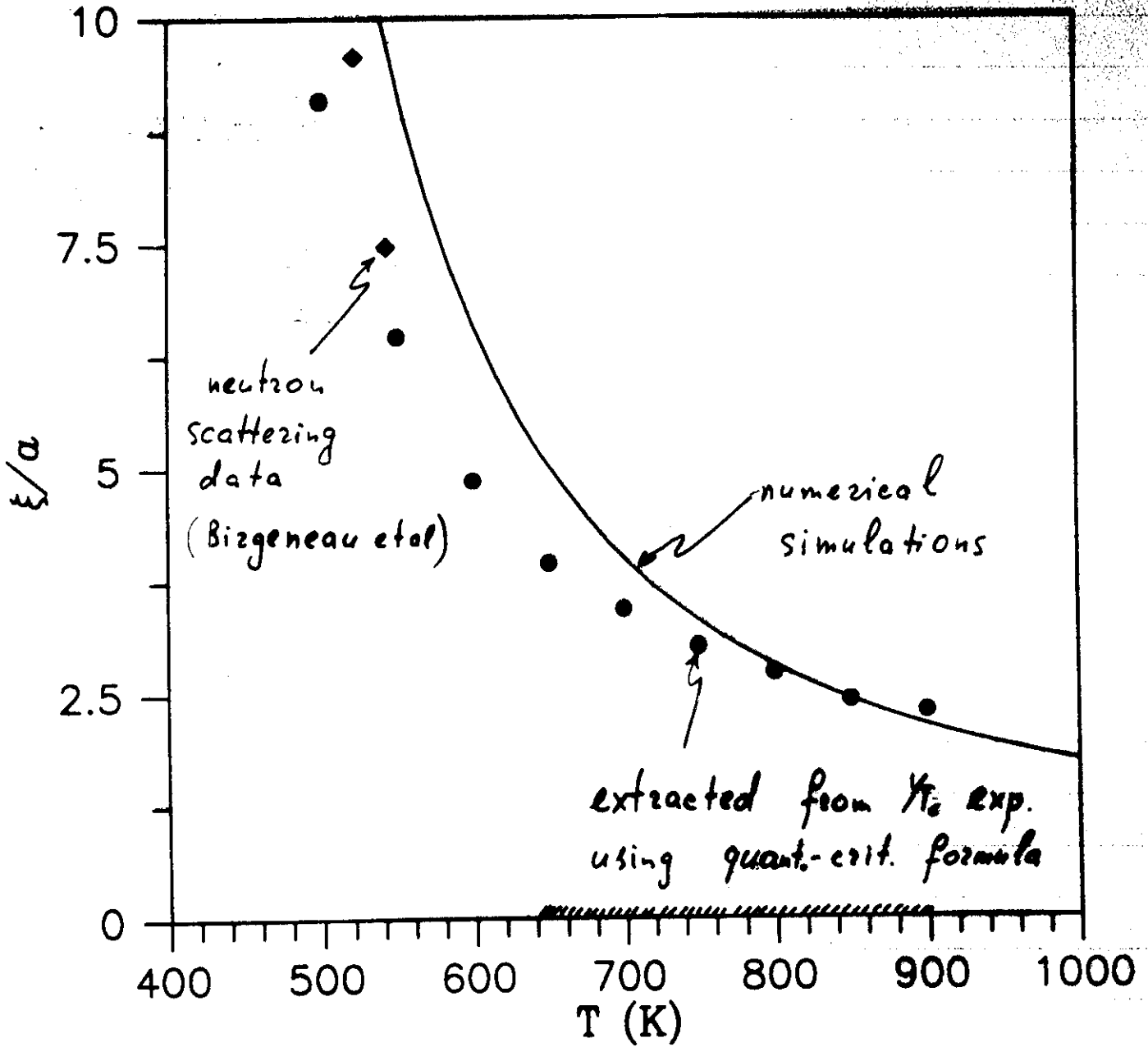
$N_0 = 0.305$ spontaneous magnetization

$N=3$ is a physical case

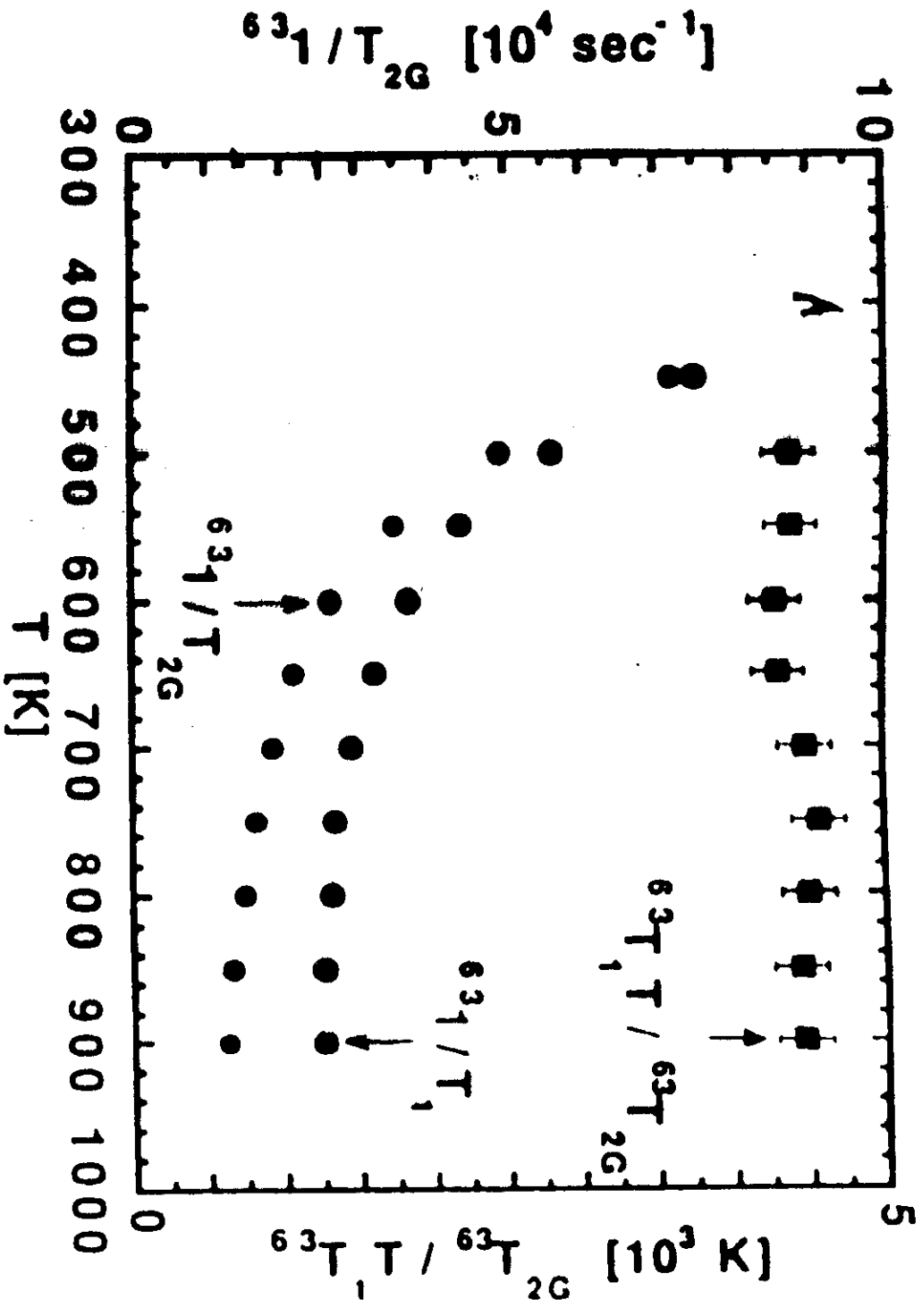
$$\frac{1}{T_2} \approx 0.546 \frac{1}{a} \times 10^4 \text{ sec}^{-1}$$

Fig 1

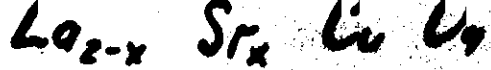
Correlation length



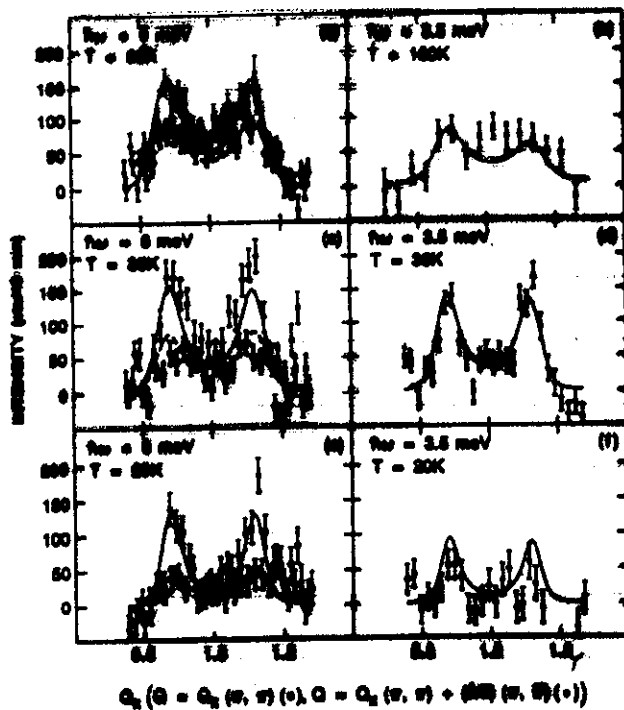
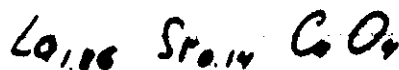
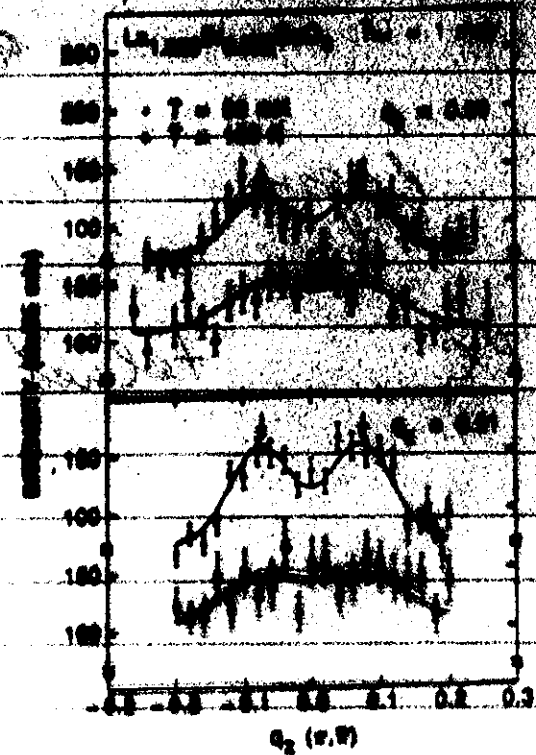
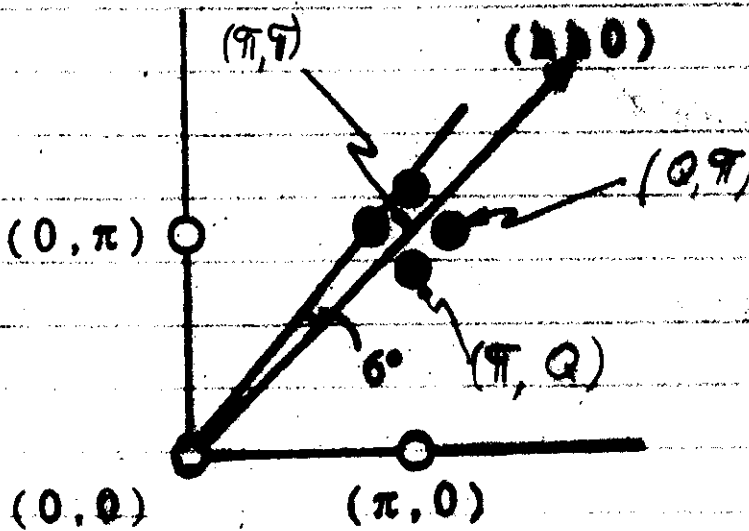
Chubukov, Sachdev & Sokol



Imai et al



$\chi''(q, \omega)$



$\delta \approx 2x$

Max in $\chi''(q, \omega)$ at $q = (\pi, \pi) \pm \delta(\pi, 0)$
 $(\pm \delta(0, \pi))$

χ'' can also be inferred from χ''

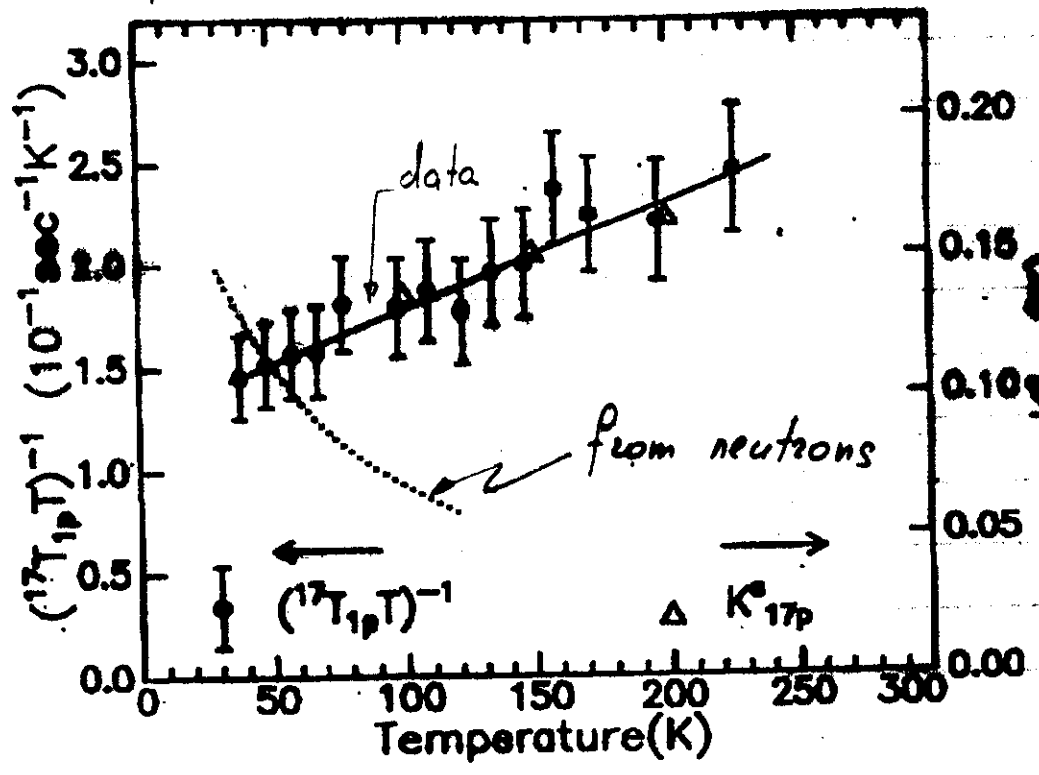
$$\frac{1}{T_2} = T \int d^3q F(q) \frac{\chi''(q, \omega)}{\omega} \Big|_{\omega \rightarrow 0}$$

$$F(q) = \begin{cases} \text{const} & \text{for } Cu \\ O(q) & \text{for } O \end{cases} \quad ; \quad F(q) \sim (\pi - q)^2 \text{ for } Cu$$

In quantum-critical region,

$\chi'' \sim 1/T$ if max in χ'' is away from (π, π)
 $\chi'' \sim T$ if max in χ'' is at (π, π) .

^{17}O



Finite doping

- $g \rightarrow g_c$
- this is not the only effect of doping
(millis)

SDW theory of 2D Hubbard model

$$\mathcal{H} = -t \sum_{\langle ij \rangle} c_{i\sigma}^\dagger c_{j\sigma} - t' \sum_{\langle ij \rangle'} c_{i\sigma}^\dagger c_{j\sigma} + U \sum_i n_{i\uparrow} n_{i\downarrow}$$

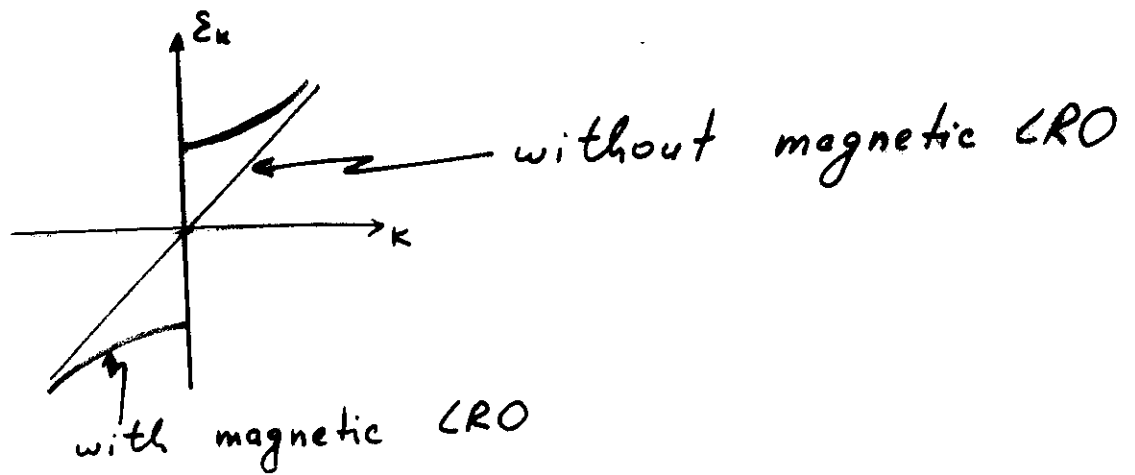
- antiferromagnetism at half-filling

$$\vec{S} = c_\alpha^\dagger \vec{\tau}_{\alpha\beta} c_\beta$$

$$\langle S_z(i) \rangle = (-1)^i \lambda$$

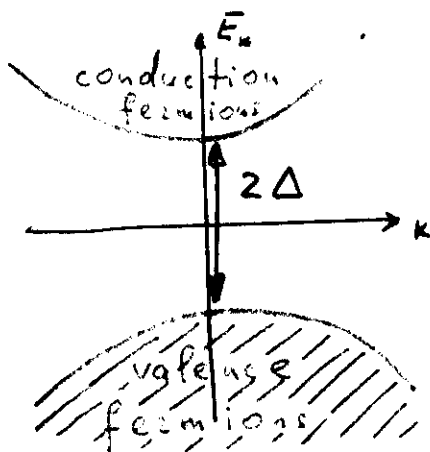
- (π, π) antiferromagnetism if $|t'| < t/\sqrt{2}$

• Electronic spectrum at half-filling



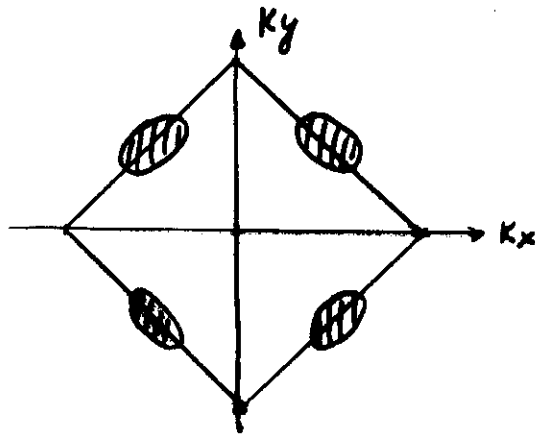
$$E_k = \pm \sqrt{\Delta^2 + 4t^2 (\cos k_x + \cos k_y)^2} - 4t' \cos k_x \cos k_y$$

$$\Delta = U \cdot \langle S_z \rangle$$



Band minima
at $(\pm \pi/2, \pm \pi/2)$ if $t' < 0$
and $|t'| < J$

(In La_2CuO_4 ,
 $t' \approx -0.2t$
 $J \approx 0.4t$)



• in the model with $t' = 0$,

hole pockets are located at $(\pm\frac{\pi}{2}, \pm\frac{\pi}{2})$

variational Monte-Carlo	Manousakis
variational wave functions	Trugman Sachdev
perturbative " $\frac{1}{5}$ " expansion	Chubukov & Muscelian

- Bosonic excitations \equiv collective modes

$$\chi(q) = \text{[diagram 1]} + \text{[diagram 2]} + \dots$$

The first diagram shows a circle with two wavy lines on the left and right sides, representing a bubble diagram. The second diagram is similar but has a vertical dashed line through the center of the circle, representing a higher-order diagram.

$$\chi(q) = \frac{\chi_0(q)}{1 - U\chi_0(q)}$$

$$\chi_0 \sim \frac{1}{U}$$

not $\sim 1/t$ as
in a metal

- $\chi(0) = \frac{1}{8J}$; $\chi(q \approx \pi) = \frac{1}{J(q-\pi)^2}$

- dynamical susceptibility \equiv 2×2 problem

$$\chi(q, q+\pi, \omega) \sim \omega$$

- systematic expansion: large number of "orbitals"

$$U \sum_i n_{i\uparrow} n_{i\downarrow} \Rightarrow -U \sum_i S_i^z$$

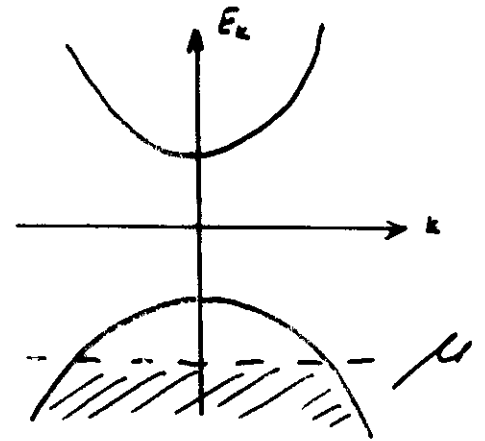
" $1/S$ " expansion
($S = 2 \times$ number of orbitals)

• at half-filling

$$\chi_0(q) = \text{Diagram}$$

•• away from half-filling

$$\chi_0(q) = \text{Diagram 1} + \text{Diagram 2}$$



Uniform susceptibility

- at $T \equiv 0$, in the ordered phase

★ $\chi \equiv 0$, $\chi_{\parallel} \equiv 0$, $\chi_{\perp} \neq 0$

★ $\chi \neq 0$

$$\chi_{\perp}^x = \chi_{\perp}^{x=0} (1 + O(x))$$

$$\chi_{\parallel}^x = \text{loop diagram} \equiv \chi_{\text{Pauli}}$$

In 2D, $\chi_{\text{Pauli}} = \sqrt{m_{\parallel} m_{\perp}} / 2\pi$, if

does not depend on carrier concentration

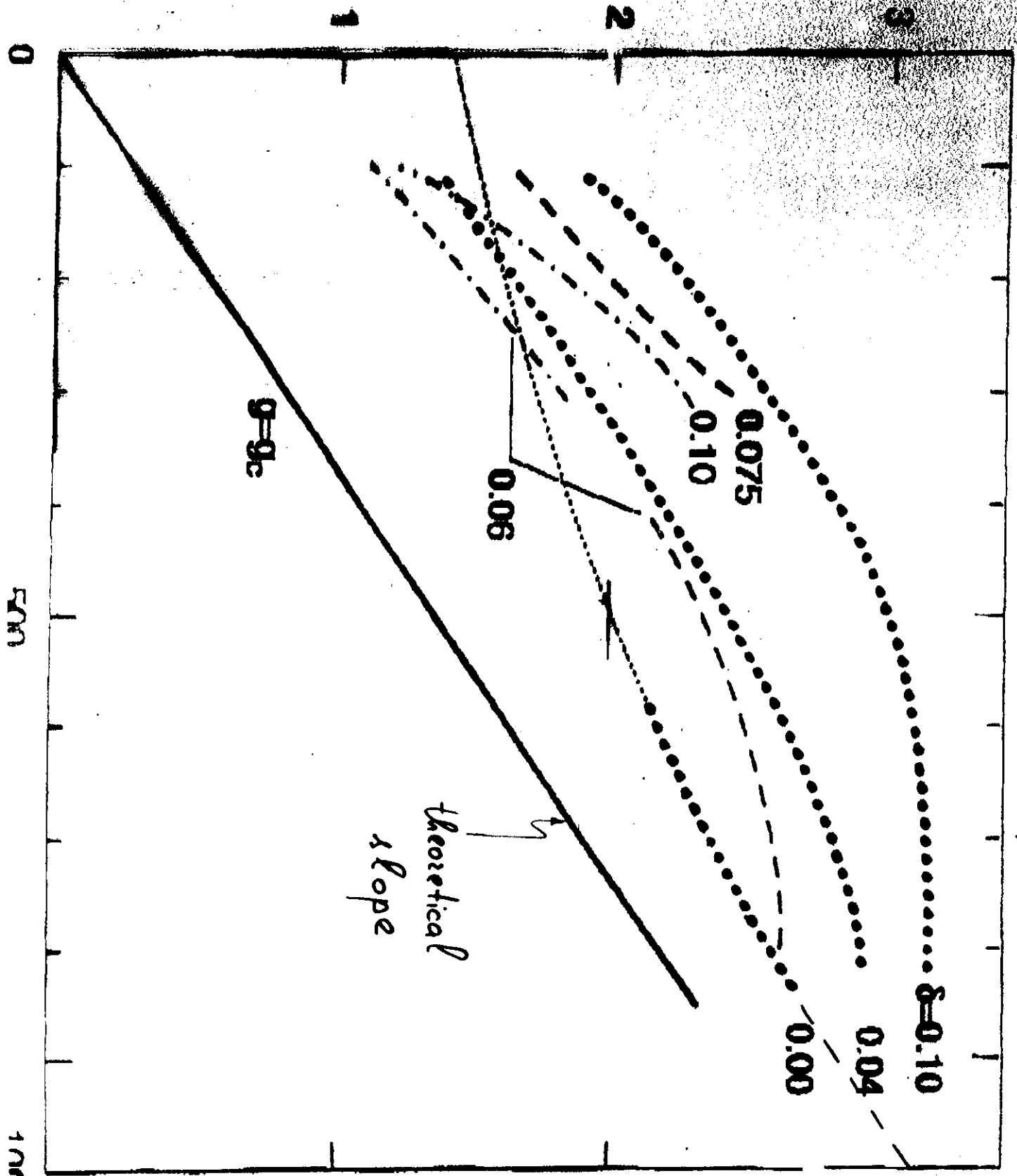
$$E_k = \Delta + \frac{k_{\parallel}^2}{2m_{\parallel}} + \frac{k_{\perp}^2}{2m_{\perp}}$$

at $T \rightarrow 0$ $\chi_{\text{tot}} = \frac{2}{3} \chi_{\perp} + \frac{1}{3} \chi_{\text{Pauli}}$

T increases

$$\chi_{\text{tot}} = \chi_{\text{spin}} + \frac{1}{3} \chi_{\text{Pauli}}$$

χ_0/μ_B^2 [states/eV-Cu]



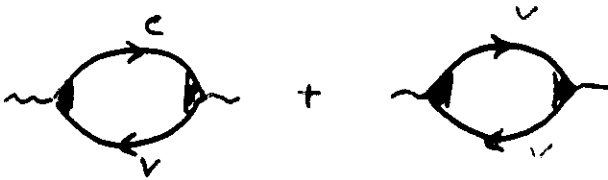
mills, 95

45

Staggered susceptibility

• $\chi_{\text{tot}}(q) = \rho_s \bar{q}^2$, $\bar{q}_i = \pi - q_i$

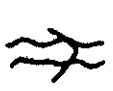
$\rho_s = \rho_s^{x=0} (1 - ?)$

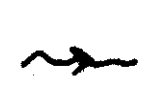
∴ $\chi_0(q) =$ 

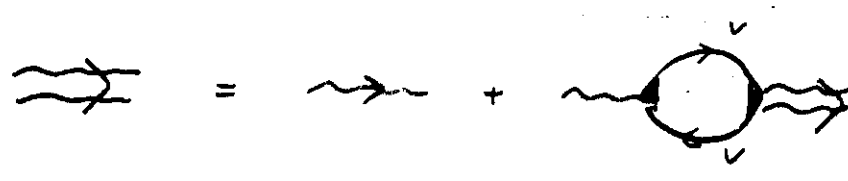
$\chi_0(q)$ has to be substituted into RPA series

Rule of the game:

valence - valence bubbles are separated by valence - conduction ones

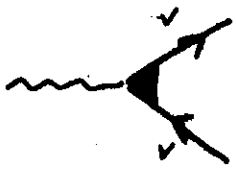
$\chi^{\text{tot}} =$ 

$\chi_{x=0}^{\text{tot}} =$ 

$\chi^{\text{tot}} =$ 

$\rho_s \bar{q}^2 = \rho_s^{x=0} \bar{q}^2 -$ 

Vertex



$$\equiv + (\bar{q}_x \sin k_x + \bar{q}_y \sin k_y)$$

- pockets at $(\pm\sqrt{2}, \pm\sqrt{2}) \Rightarrow |\sin k_i| = 1$

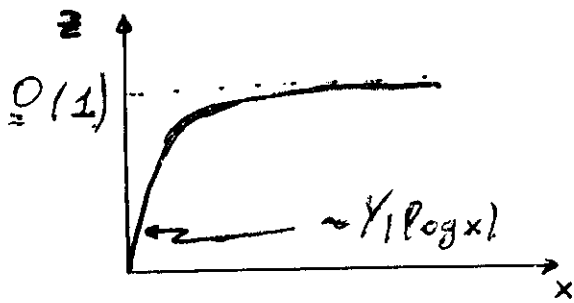
$$\rho_s = \rho_s^{x=0} - \lambda t^2 \chi_{\text{Pauli}}$$

does not
depend on carrier
concentration

$$\rho = \rho^{x=0} (1 - z)$$

• mean-field $z = \frac{24}{\pi} \sqrt{m_{\parallel} m_{\perp}} \sim O(\frac{4}{3}) \gg 1$

• with self-energy & vertex corrections + $U \rightarrow T$ (scattering amplitude)



In any event, ρ_s rapidly decreases with doping.

- $\rho_s = \rho_s^{x=0} (1 - z)$

$$N_0 = N_0^{x=0} (1 - \underline{Q}(x))$$

$$\chi_{\perp} = \chi_{\perp}^{x=0} (1 - \underline{Q}(x))$$

- $z \equiv z(\omega)$

$$z(\omega) = z(\omega=0) \left[1 - \left(\frac{\delta^2}{\delta^2 + 1} \right)^{1/2} \right]$$

$$\delta^2 = \frac{\omega^2 m_{\parallel} m_{\perp}}{\bar{q}^2 p_F^2}$$

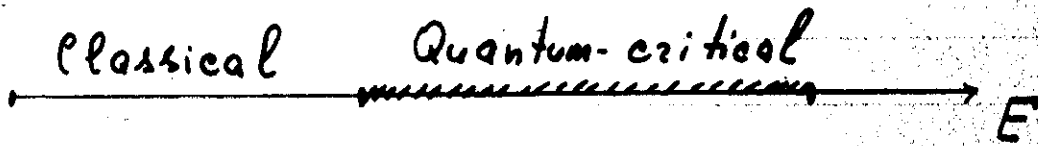
At spin-wave frequencies,

$$\omega = c q \Rightarrow \delta^2 \sim \frac{1}{p_F^2} \sim \frac{1}{x} \gg 1$$

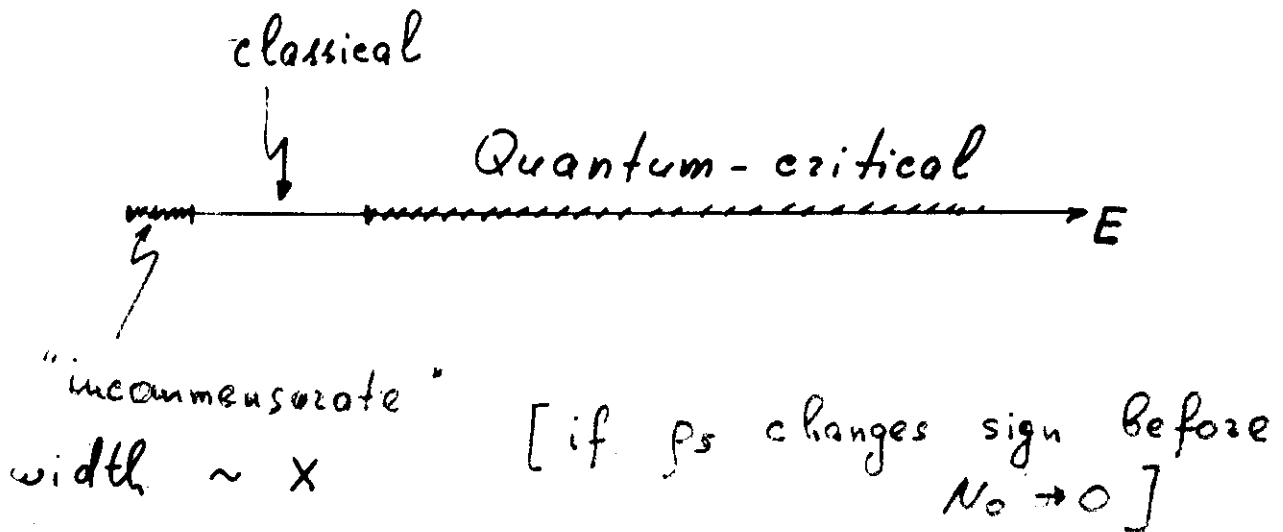
then $z(\omega) \sim \underline{Q}(x) !$

We have new scale $\sim \underline{Q}(x)$

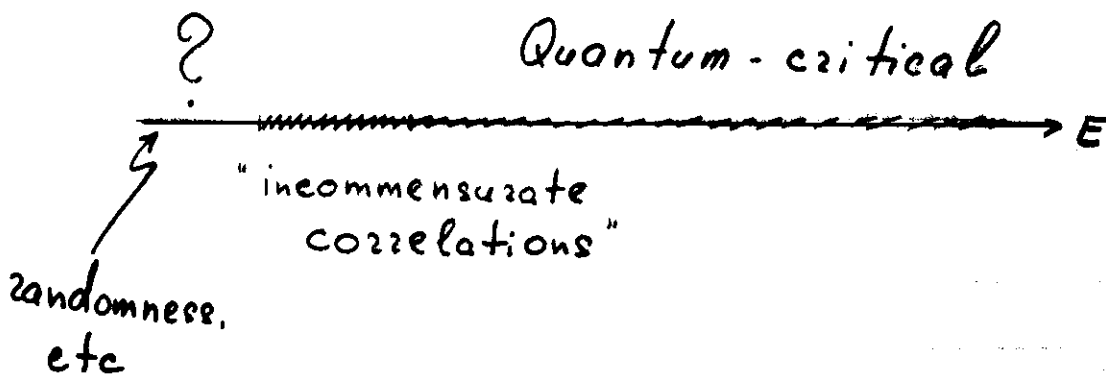
- at half-filling



- at finite doping



- above 4% doping



$$\chi''(\omega) \sim I(|\omega|) F(\omega/T)$$

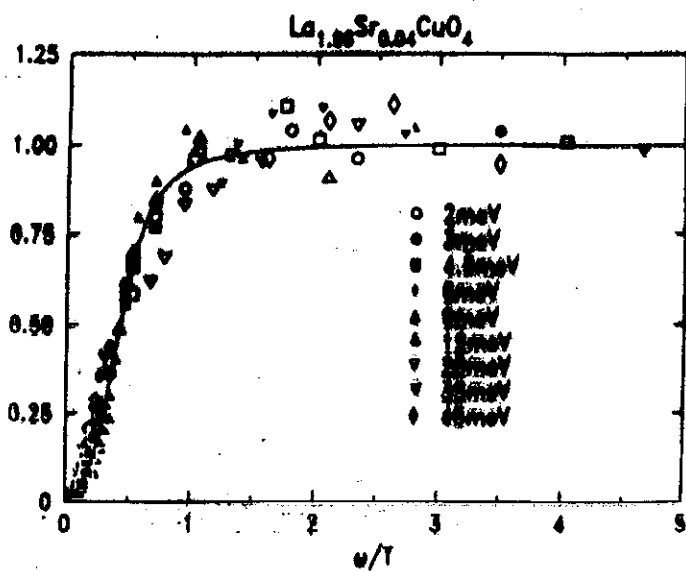


Figure 5: Neutron scattering results for the scaling function F from Ref. [15]

Keimer et al

In a pure system, $I(|\omega|) \sim \omega^? = \text{const}$

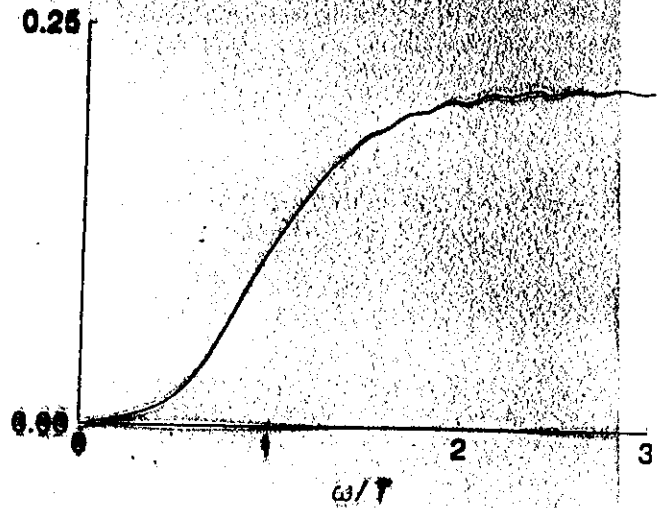


Figure 4: The imaginary part of the universal local susceptibility F , for the same model as in the previous figure. We have $F(y) = y^{-2} / (2 \int_0^y dx x^{-2})$. The oscillations at large y are due to a finite step-size in the momentum integrations.

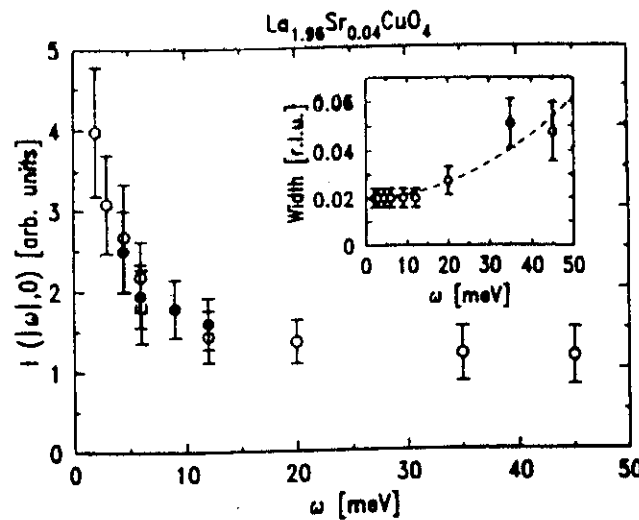


Figure 6: Neutron scattering results for the normalization factor I from Ref. [15]

Conclusions

- we found the new low-temperature region in quantum Heisenberg antiferromagnets, which is governed by the quantum-critical fixed point
- theoretical results for uniform susceptibility, static structure factor, local susceptibility and spin-lattice relaxation rates, T_1 and T_2 , agree well with the experimental data
- quantum-critical region stretches to lower T with doping.

REFERENCES

- [1] Q. Si, Y. Zha, K. Levin and J.P. Lu, Phys. REv B **47**, 9055 (1993) and references therein.
- [2] A. Sokol and D. Pines, Phys. REv. Lett **71**, 2813 (1993).
- [3] S. John and P. Voruganti, Phys. Rev. B **43**, 10815 (1991); S. John and P. Voruganti, and W.Goff, Phys. Rev. B **43**, 13365 (1991).
- [4] A.V.Chubukov and D.M.Frenkel, Phys. Rev. B **46**, 11884 (1992).
- [5] H.Monien and K.S.Bedell, Phys. Rev. B **45**, 3164 (1992).
- [6] J.R.Schrieffer, X.G.Wen, and S.C.Zhang, Phys. Rev. B **39**, 11663 (1989).
- [7] B.I.Halperin and P.C.Hohenberg, Phys. Rev. **188**, 898 (1969); D.Forster, *Hydrodynamic Fluctuations, Broken Symmetry, and Correlation Functions* (Benjamin/Cummings, Reading, MA, 1975)
- [8] I.Affleck and F.D.M.Haldane, Phys. Rev. B **36**, 5291 (1987).
- [9] B. I. Shraiman and E. D. Siggia, Phys. Rev. Lett. **60**, 740 (1988); **61**, 467 (1988).
- [10] C. L. Kane, P. A. Lee, and N. Read, Phys. Rev. B **39**, 6880 (1989).
- [11] A. Singh and Z. Tešanović, Phys. Rev. B **41**, 11457 (1990).
- [12] E. Dagotto, R. Joynt, A. Moreo, S. Bacci and E. Gagliano, Phys. Rev B **41**, 9049 (1990); M. Boninsegni and E. Manousakis, Phys. Rev. B **43**, 10353 (1991).
- [13] S. Trugman, Phys. Rev B **37**, 1597 (1988); S. Sachdev, Phys. Rev B **39**, 12232 (1989).
- [14] R.G. Gooding, K.J.E. Vos and P.W. Leung, unpublished.
- [15] A.V. Chubukov and K. Musaelian, unpublished
- [16] A.V. Chubukov and K. Musaelian, unpublished